Electrostatic potential of ferroelectric $PbTiO_3$: Visualized electron polarization of Pb ion

Hiroshi Tanaka
Department of Materials Science, Shimane University, 1060 Nishi-kawatsu-cho, Matsue, Shimane 690-8504, Japan

Yoshihiro Kuroiwa
Department of Physical Science, Hiroshima University, 1-3-1 Kagamiyama, Higashi-Hiroshima, Hiroshima 739-8526, Japan

Masaki Takata
RIKEN SPring-8 Center, Sayo-gun, Hyogo 679-5198, Japan
(Received 18 July 2006; published 16 November 2006)

A different method is proposed to evaluate the electrostatic potential and electric field from x-ray diffraction data by using maximum entropy method. The efficiency of the method is revealed in the application to a ferroelectric material $PbTiO_3$. Visualized electrostatic potential and electric field on the charge density distribution give a direct evidence for the dipolar polarization of the Pb ion. They show close agreement with results by *ab initio* calculations.

DOI: 10.1103/PhysRevB.74.172105 PACS number(s): 77.80.−e, 05.70.−a, 61.10.Nz, 77.84.Dy

$BaTiO_3$ and $PbTiO_3$ are typical ferroelectric materials with a perovskite-type structure. For a long time, their ferroelectric properties have been studied mainly on the basis of displaced ion models and classical electromagnetics, since Slater analyzed the ferroelectricity of $BaTiO_3$ by the geometrical configuration of atoms and local electric field.[1]

In the 1990s, the electronic structures of these materials were studied extensively by *ab initio* calculations.[2–6] Then it was revealed that the electronic structure plays important roles in ferroelectric properties of these materials. Cohen pointed out that there exists electron orbital hybridizations between Pb and O orbitals as well as between Ti and O orbitals in $PbTiO_3$, which induce the covalency between Pb and O ions and the polarization of Pb ion. In $BaTiO_3$, in contrast, the hybridization between Ba and O orbitals and resultant polarization of Ba ion are not observed. He concluded that the hybridization stabilizes the tetragonal structure of $PbTiO_3$ and enhances its ferroelectricity compared with that of $BaTiO_3$.[2,3]

Kuroiwa *et al.* showed the first experimental evidence for the Pb-O covalency in tetragonal $PbTiO_3$ by using maximum entropy method (MEM) analysis of powder diffraction data obtained by synchrotron radiation.[7] They also found that there is a charge transfer from four O ions to a Pb ion by 0.9 electrons associated with the cubic-tetragonal phase transition.

The MEM analysis was proposed by Collins.[8] The method enables us to reproduce electronic charge density distributions with high resolution from a limited number of diffraction data, and has been applied to a wide variety of materials.[9,10] It is now applicable to huge systems, such as proteins, coupled with the recent parallel processing in computation and the fast Fourier transform (FFT) technique.[11] In this report, we have extended the method to evaluate the electrostatic potential.

Several approaches have been proposed, which evaluate the electrostatic potential from experimental x-ray diffraction data. For example, Bertaut[12] and Stewart[13] proposed a formalism to evaluate the potential directly from the experimental structure factors by the Fourier transformation. The summation in reciprocal space, however, suffers from Gibbs's oscillation, unless enough number of structure factors is available to attain to the converged potential. Su and Coppens evaluated the electrostatic potential of deuterated benzene[14] based on the multipole expansion,[15] in which the electron charge density is expanded into a series of spherical harmonic functions. A merit of the method is that we can lift a molecule out of the crystal.[16] Difficulties are originated from the complex procedure in evaluation and the ambiguity in how to redistribute the electron charge to each constitutive atom.

In this study, we propose an alternative method to evaluate the electrostatic potential by using the maximum entropy method (MEM) together with Ewald's technique.[17] The electrostatic potential $U(\boldsymbol{r})$ in a solid consists of the contributions from the nucleus charge and the electron charge

$$U(\boldsymbol{r}) = U_{\mathrm{nuc}}(\boldsymbol{r}) + U_{\mathrm{ele}}(\boldsymbol{r}). \tag{1}$$

The potential due to the electron charge can be rewritten by the summation in the reciprocal lattice $\boldsymbol{G}$ as $U_{\mathrm{ele}}(\boldsymbol{r}) = -4\pi\Sigma_{\boldsymbol{G}}\tilde{\rho}(\boldsymbol{G})\exp(i\boldsymbol{G}\boldsymbol{r})/|\boldsymbol{G}|^2$, where $\tilde{\rho}(\boldsymbol{G})$ is the Fourier component of the electronic charge density $\rho(\boldsymbol{r})$. Since the structure factor $F(\boldsymbol{G})$ is expressed as $F(\boldsymbol{G}) = \Omega\tilde{\rho}(\boldsymbol{G})$ with the volume Ω in the real space, the potential due to electron charge can be calculated by

$$U_{\mathrm{ele}}(\boldsymbol{r}) = -4\pi\sum_{\boldsymbol{G}} \frac{F(\boldsymbol{G})\exp(i\boldsymbol{G}\boldsymbol{r})}{\Omega|\boldsymbol{G}|^2}. \tag{2}$$

However, it is normally difficult to observe sufficient number of reflections to get a converged value for Eq. (2). Analyzing x-ray diffraction data by MEM has an advantage to overcome the problem. By using MEM, we can extrapolate the structure factor up to the large value of $|\boldsymbol{G}|$ necessary for the convergence of Eq. (2), which reproduce a smooth and accurate charge density distribution of electrons. Then, we employ the extrapolated structure factor $F_{\mathrm{MEM}}(\boldsymbol{G})$ instead of observed one in the following calculation. Namely, we approximate

$$F(\boldsymbol{G}) \simeq F_{\mathrm{MEM}}(\boldsymbol{G}). \tag{3}$$

This is the key point of our method.

On the other hand, the electrostatic potential due to the nucleus charge can be evaluated by ordinary Ewald's method. Combining Ewald's method with Eqs. (1)–(3), we get a formulation to evaluate electrostatic potential

$$U(\boldsymbol{r}) = 4\pi \sum_{\boldsymbol{G}} \frac{\sum_t Z_t \exp(-|\boldsymbol{G}|^2/\eta^2 - i\boldsymbol{G}\boldsymbol{R}_t) - F_{\mathrm{MEM}}(\boldsymbol{G})}{\Omega|\boldsymbol{G}|^2} \times \exp(i\boldsymbol{G}\boldsymbol{r}) + \sum_{\boldsymbol{l}} \sum_t \frac{Z_t}{|\boldsymbol{r}-\boldsymbol{l}-\boldsymbol{R}_t|} \mathrm{erfc}(\eta|\boldsymbol{r}-\boldsymbol{l}-\boldsymbol{R}_t|), \tag{4}$$

where $\boldsymbol{R}_t$, Z_t, and $\boldsymbol{l}$ are position vector of the tth basis atom relative to the lattice point, atomic number of the tth basis atom, and lattice point vector, respectively. The function $\mathrm{erfc}(x)$ is the complementary error function. The only parameter in this method is the variable η, which should be chosen so that both summations in real and reciprocal lattices converge rapidly. The final result does not depend on the choice of η, if the summation is taken over enough number of lattice points in real and reciprocal spaces. An advantage of this method should be emphasized that everybody can evaluate the electrostatic potential without any experience unlike conventional methods, such as the multipole expansion.

Although there is a singularity at $\boldsymbol{G}=0$ in the first term on right hand side of Eq. (4), it is removable because $Z_t\exp(-|\boldsymbol{G}|^2/\eta^2 - i\boldsymbol{G}\boldsymbol{R}_t)$ and $F_{\mathrm{MEM}}(\boldsymbol{G})$ cancel out each other at $\boldsymbol{G}=0$.

In the present formulation, the thermal vibration of nucleus is not considered. However, it is straightforward to take the effect into account within the harmonic approximation in our formulation. It requires only a slight modification of Ewald's sum because the distribution of nucleus charge is given by a Gaussian type function whether it is isotropic or not.

Taking the gradient of Eq. (4), we can also evaluate the electric field as

$$\boldsymbol{E}(\boldsymbol{r}) = 4\pi i \sum_{\boldsymbol{G}} \frac{F_{\mathrm{MEM}}(\boldsymbol{G}) - \sum_t Z_t \exp(-|\boldsymbol{G}|^2/\eta^2 - i\boldsymbol{G}\boldsymbol{R}_t)}{\Omega|\boldsymbol{G}|} \times \exp(i\boldsymbol{G}\boldsymbol{r}) \frac{\boldsymbol{G}}{|\boldsymbol{G}|} + \sum_{\boldsymbol{l}} \sum_t Z_t \left(\frac{\mathrm{erfc}(\eta|\boldsymbol{r}-\boldsymbol{l}-\boldsymbol{R}_t|)}{|\boldsymbol{r}-\boldsymbol{l}-\boldsymbol{R}_t|^2} + \frac{2\eta \exp(-\eta^2|\boldsymbol{r}-\boldsymbol{l}-\boldsymbol{R}_t|^2)}{\sqrt{\pi}|\boldsymbol{r}-\boldsymbol{l}-\boldsymbol{R}_t|} \right) \frac{\boldsymbol{r}-\boldsymbol{l}-\boldsymbol{R}_t}{|\boldsymbol{r}-\boldsymbol{l}-\boldsymbol{R}_t|}. \tag{5}$$

We applied the above method to tetragonal $PbTiO_3$ at 300 K and evaluated both the electrostatic potential and electric field. The diffraction data described in Ref. 7 were employed in the present analysis. It includes 233 independent reflections up to $\boldsymbol{G}_{\max}=(3,2,8)$. They exist within a spherical area with the radius of $|\boldsymbol{G}_{\max}|$ in the reciprocal lattice.

The MEM analysis was carried out with the unit cell divided into $64\times64\times64$ pixels. This provide us extrapolated values for structure factor $F_{\mathrm{MEM}}(\boldsymbol{G})$ within a tetragonal area in the reciprocal lattice specified by $\boldsymbol{G}=(h,k,l)$ with $-31 \le h,k,l \le 31$. The number of them is large enough to obtain the converged value for the summation over $\boldsymbol{G}$ in Eq. (4).

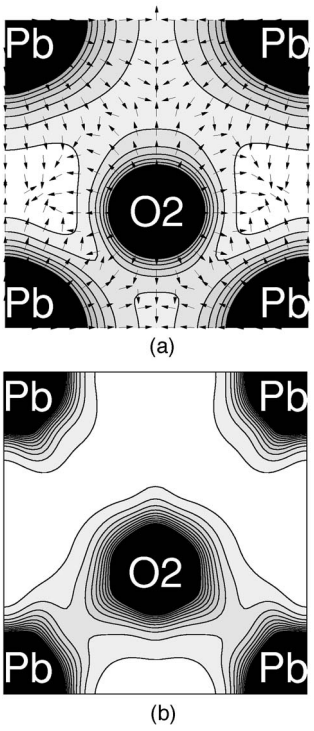

FIG. 1. (a) Contour plot of electrostatic potential on the (100) plane. The contour lines are drawn from −1.4 to 0.2 e/Å with interval of 0.2 e/Å. The direction of electric field at each point is also indicated by arrows. (b) Contour plot of electronic charge density on the (100) plane. The contour lines are drawn from 0.2 to 2.0 e/Å^3 with the interval of 0.2 e/Å^3.

Although the MEM analysis gives the extrapolated values for the structure factor, it does not increase the spatial resolution of resulting charge density map. The MEM derives the most smooth charge density, which is free from unphysical Gibbs's oscillation and reproduces the obtained structure factor. The spatial resolution of the obtained charge density is determined by $2\pi/|\boldsymbol{G}_{\max}|$, which is ~0.5 Å in the present case. The value of charge density at each point is regarded to be averaged one over the volume $0.5\times0.5\times0.5$ Å^3 around the point.

There are crystallographically different two O ions in tetragonal $PbTiO_3$. One (O1) is surrounded by Pb ions in a plane perpendicular to the c axis, and the other (O2) surrounds Ti ion in another plane perpendicular to the c axis.

Figure 1(a) shows the contour plot of electrostatic potential on the (100) plane including Pb and O2 ions. The contour plot of charge density distribution is also shown in Fig. 1(b) for comparison. As it was already reported, the charge density is significantly high between Pb and O2 ions [Fig. 1(b)], which indicates the existence of orbital hybridization between these atoms. The tail part of the electrostatic potential (low potential area) spreads wider area around the Pb ion than around the O2 ion [Fig. 1(a)]. This is because Pb is cation and the number of electrons is less than that of

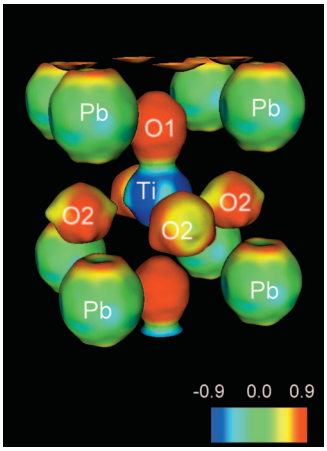

FIG. 2. (Color) Isosurface of charge density for $PbTiO_3$ at 0.86 e/Å^3. It is colored by the value of electrostatic potential from −0.9 e/Å (red) to 0.9 e/Å (blue).

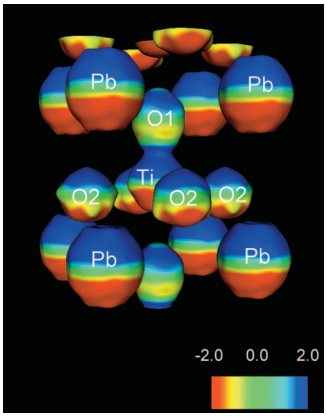

FIG. 3. (Color) Isosurface of charge density for $PbTiO_3$ at 1 e/Å^3. It is colored by the amplitude of z component of the electric field from −2.0 e/Å^2 (red) to 2.0 e/Å^2 (blue).

nucleus charge. Then the valence electrons cannot screen the potential due to nucleus charge away from the nucleus.

In general, it is expected that the spatial resolution of the electrostatic potential is better than that of charge density because the former is evaluated by integrating the function of the latter. In practice, the obtained electrostatic potential is smooth and almost spherically symmetric around each atom position compared with the charge distribution as shown in Fig. 1(a).

The directions of electric field at each point are also plotted in Fig. 1(a) by arrows. They perpendicularly cross the contour lines of electrostatic potential. We will discuss the characteristics of electric field in detail later.

The contour lines of charge density around the Pb ion shows oval shape stretched in the c axis direction, which implies polarization of electronic charge at atomic level. This agrees well with the *ab initio* calculation.[3] Corresponding to this, the contour lines of potential around Pb ion also shows oval shape but stretched in the direction perpendicular to the c axis.

We can see the polarization of electronic charge in $PbTiO_3$ more clearly in Fig. 2. The isosurface of the electronic charge density is colored by the value of electrostatic potential from −0.9 e/Å (red) to 0.9 e/Å (blue) in the figure. The isosurface around O ions is colored by red, indicating negative potential, because O is anion. On the other hand, the isosurface around Ti ion is colored by blue, indicating positive potential, because Ti is cation.

The most part of isosurface around Pb ion is colored by green. Note that the head area of the surface is red, while the bottom area is yellow. This means that the center of electronic charge is shifted toward the c-axis direction relative to the center of nucleus charge, which is evident for the atomic level polarization of Pb ion. Our results support the argument by Cohen[3] that the Pb and O ions make hybridized orbital, which induces atomic level polarization of the Pb ion.

In order to show the efficiency of our method, we also illustrated the isosurface colored by the amplitude of z components of electric field in Fig. 3, which can be compared with that obtained by the *ab initio* calculation by Cohen (Fig. 3 in Ref. 3). We cannot compare the shape of the isosurface between our result and the *ab initio* calculation because our charge density includes the core charge density while that obtained by *ab initio* calculation does not. The distribution of electric field obtained in the present analysis, however, shows close agreement with that of the *ab initio* calculation.

In summary, we developed a method to visualize the electrostatic potential and electric field on the electron charge density distribution by combining the MEM and Ewald's method. An advantage of the method is that we can conduct analysis without any special experience. It was applied to a typical ferroelectric material $PbTiO_3$. The obtained electrostatic potential gives an experimental evidence for the polarization of Pb ion at atomic level. The electric field was also evaluated by the method. The obtained field shows close agreement with that by the *ab initio* calculation. These facts mean that our method is efficient for the experimental analysis of the electrostatic potential in the crystalline material.

Part of this work has been supported by the Grant-in-Aid for Scientific Research from the Ministry of Education, Culture, Sports, Science, and Technology, Japan.

[1] J. C. Slater, Phys. Rev. **78**, 748 (1950).
[2] R. E. Cohen and H. Krakauer, Phys. Rev. B **42**, 6416 (1990).
[3] R. E. Cohen, Nature (London) **358**, 136 (1992).
[4] R. D. King-Smith and D. Vanderbilt, Phys. Rev. B **47**, 1651 (1993).
[5] W. Zhong, R. D. King-Smith, and D. Vanderbilt, Phys. Rev. Lett. **72**, 3618 (1994).
[6] W. Zhong, D. Vanderbilt, and K. M. Rabe, Phys. Rev. B **52**, 6301

(1995).
[7] Y. Kuroiwa, S. Aoyagi, A. Sawada, J. Harada, E. Nishibori, M. Takata, and M. Sakata, Phys. Rev. Lett. **87**, 217601-1 (2001).
[8] D. M. Collins, Nature (London) **298**, 49 (1982).
[9] M. Sakata and M. Sato, Acta Crystallogr., Sect. A: Found. Crystallogr. **A46**, 263 (1990).
[10] M. Takata, E. Nishibori, and M. Sakata, Z. Kristallogr. **216**, 71 (2001), and references there in.
[11] H. Tanaka, M. Takata, E. Nishibori, K. Kato, T. Iishi, and M. Sakata, J. Appl. Crystallogr. **35**, 282 (2002).
[12] E. F. Bertaut, J. Phys. Chem. Solids **39**, 97 (1987).
[13] R. F. Stewart, Chem. Phys. Lett. **65**, 335 (1976).
[14] Z. Su and P. Coppens, Acta Crystallogr., Sect. A: Found. Crystallogr. **48**, 188 (1992).
[15] N. K. Hansen and P. Coppens, Acta Crystallogr., Sect. A: Cryst. Phys., Diffr., Theor. Gen. Crystallogr. **34**, 909 (1978).
[16] P. Coppens, Z. Su, and P. J. Becker, *International Tables for Crystallography*, 2nd ed., edited by A. J. C. Willson and E. Prince (Dordrecht: Kluwer Academic Publishers, 1999), Vol. C, p. 713.
[17] P. P. Ewald, Ann. Phys. **64**, 253 (1921).